by 3 before entering them in Table II.

The spin–lattice relaxation times T_1 were measured by inversion–recovery (90° pulse = 6.8 μs) at 302 K on the same sample (not degassed) used for saturation transfer studies. An equilibration delay of 30 s was used, nine different recovery times, and four transients per FID. Peak heights were fit by nonlinear least-squares analysis to the three-parameter function. $I_z(t) = A - B\exp(-t/T_1)$ to determine A, B, T_1. The values of A and B were 0.97 ± 0.02 and −1.92 ± 0.02, respectively, for all fits.

Resolution enhancement via the Lorentz-to-Gaussion line-shape transformation[28] was used extensively to extract all possible information from the spectra. The natural line width of signals and the relatively broad wings of the Lorentzian line shape normally limit the resolution in NMR spectra. Multiplication of the original free induction decay (FID) with an appropriate double exponential function can remove the Lorentzian component and introduce a narrower Gaussian line shape. Figure 3 shows the result of a rather strong enhancement which has been optimized for the aromatic signals (Figure 3A) to produce a pure Gaussian line shape without wings. For the methyl signals an over-enhancement has been purposely used to clarify the multiplet structure, resulting in a "negative" Lorentzian component giving the negative wings in the spectrum. For integration purposes it is mandatory that the enhancement be performed in such a way as to avoid negative line shapes (Figure 6). The resolution achievable in this way is limited only by the digital resolution and the signal-to-noise ratio in the original FID.

Integration was performed using the computer software routines that allow accurate baseline correction for individual peaks, precise definition of integration limits, and digital printout of integral values. The integrals were normalized either by setting the lowest field aromatic proton or the total OH integral to 1.00. Increasing degrees of resolution enhancement were applied and phase was adjusted by optimizing the flatness and continuity of the baseline across the spectrum. For the OH signal of **7** and **8** some trails were made by dividing the integral in the exact center between the two signals; other trials involving further resolution enhancement allowed impurity peaks to be integrated separately. The results of all trials are summarized in Table III. The integration limits to the left and right of the OH signals were varied from trial to trail to give an indication of the uncertainties involved. The maximum variation that could be produced in a "reasonable" way was ±2%. In general, the methyl signals could be more reproducibly integrated since their line shape was narrower and impurity peaks could be better avoided. Integral tests made with **5** demonstrated conclusively that the integration techniques used can give an absolute accuracy of ±0.005 proton, which is the best one can expect when ^{13}C-satellites cannot be included in each integral.

Acknowledgment. We are indebted to Professor H. Schwarz and to Dr. M. Spraul for preliminary integration experiments and to Professor F. A. L. Anet for discussions. This work was supported by a grant from the United States–Israel Binational Science Foundation (BSF), Jerusalem, Israel, to which we are grateful.

Registry No. 5, 26905-20-4; **7a**, 88180-82-9; **7b**, 88180-83-0; **8a**, 88180-84-1; **8b**, 88200-35-5; **9a**, 88180-86-3; **9b**, 88180-87-4; **10a**, 97571-63-6; **10a**-α-*d*, 97571-64-7; **10b**, 97571-65-8; **10b**-α-*d*, 97571-66-9; **11**, 88180-90-9; **12**, 77787-79-2.

(28) Ernst, R. R. *Adv. Magn. Reson.* **1966**, *2*, 1–135.

Hemiacetal Formation with a Phenol Nucleophile: Simple Proton Transfers as Rate-Limiting Steps

Robert A. McClelland,*† David B. Devine,† and Poul E. Sørensen*‡

Contribution from the Department of Chemistry, University of Toronto, Toronto, Ontario, Canada M5S 1A1, and the Chemistry Department A, The Technical University of Denmark, DK-2800, Lyngby, Denmark. *Received February 4, 1985*

Abstract: A kinetic study is reported of the reversible cyclization in cacodylic acid buffers (pH 5.3–6.5) of (*Z*)-2′-hydroxy-4-methoxy-α-methylchalcone (C) to its cyclic hemiacetal isomer 2-hydroxy-2-(4-methoxyphenyl)-3-methylflav-3-ene (B). Rate–buffer plots for experiments at constant pH exhibit a complex curvature. It is proposed that there are three regions of behavior: very dilute buffers, with a steep increase in rate with increasing buffer concentration; dilute to moderately concentrated buffers, where the rate continues to rise but not nearly so steeply; and very concentrated buffers, where the rate levels. A mechanism is proposed with both the chalcone anion C^- and hemiacetal anion B^- as intermediates $C \rightleftarrows C^- \rightleftarrows B^- \rightleftarrows B$. A kinetic analysis is conducted using the measured equilibrium constant for cyclization, $K = [B]/[C] = 4$, the measured acidity constant for chalcone ionization, $pK_C = 9.1$, and an estimated acidity constant for hemiacetal ionization, $pK_B \approx 12.0$. Consistent with the two breaks in the buffer dilution plots, this analysis establishes that at some buffer concentration each step in the reaction is (mainly) rate limiting, the first step $C \rightleftarrows C^-$ in very dilute buffers, the third step $B^- \rightleftarrows B$ in more concentrated buffers, and the second step $C^- \rightleftarrows B^-$ in very concentrated buffers. The proton-transfer steps are rate limiting in dilute buffers because the anion equilibration is extremely rapid. The changes in the rate-limiting step arise because of the acceleration of the proton transfers due to participation of the buffer. A comparison with the formation/breakdown of other hemiacetals is presented. The principal difference of the chalcone system is the uncoupling of both proton transfers from C–O bond making or breaking. The factor responsible for this appears to be the increased stability of the phenoxide nucleophile/leaving group.

Several recent investigations have provided evidence[1-3] for a class "n" mechanism[4] in the general-base-catalyzed[5] addition of water and alcohols to aldehydes (eq 1). This involves, in the addition direction, a proton transfer from the water or alcohol nucleophile to the catalyzing base coupled with C–O bond formation. The second proton transfer, which is required for the

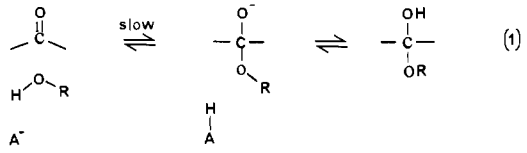

(1)

† University of Toronto.
‡ The Technical University of Denmark.

(1) Funderburk, L. H.; Aldwin, L.; Jencks, W. P. *J. Am. Chem. Soc.* **1978**, *100*, 5444–5459.
(2) McClelland, R. A.; Coe, M. *J. Am. Chem. Soc.* **1983**, *105*, 2719–2725.
(3) Sørensen, P. E.; Jencks, W. P. *J. Am. Chem. Soc.*, submitted.
(4) Jencks, W. P. *Acc. Chem. Res.* **1976**, *9*, 425–432.
(5) Bell, R. P. *Adv. Phys. Org. Chem.* **1966**, *4*, 1–29.
(6) (a) Hemiacetals and hydrates are more acidic than simple alcohols[6b] because of the acid-strengthening effect of the additional oxygen atom present in the former. (b) Hine, J.; Koser, G. F. *J. Org. Chem.* **1971**, *36*, 1348–1351.

0002-7863/85/1507-5459$01.50/0

overall reaction, follows and is a fast step. In the reverse direction equilibrium deprotonation precedes a rate-determining general-acid-catalyzed breakdown of the anion. The exact reason the reaction follows this course is not clear, but in simple terms, it can be argued that this mechanism avoids the anion RO^-, the less stable of the two anionic forms that are possible.

In this paper we analyze the base catalysis of the equilibration of the *cis*-chalcone C with its cyclic hemiacetal isomer B (eq 2).

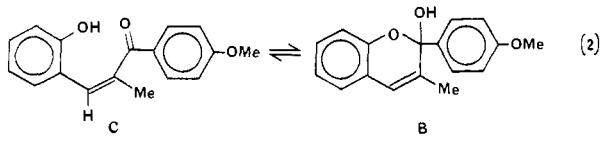

(2)

This system has a phenol nucleophile/leaving group and thus represents the situation where the anion derived from the nucleophile is more stable. Also of interest is the speed of the equilibration, a preliminary investigation[7] with a slightly different compound[8] giving a catalytic coefficient for hydroxide ion of the order of 10^{10} M^{-1} s^{-1}. A number of this magnitude implies a diffusion-limited reaction, as verified in this study. It is also of interest that the chalcone and hemiacetal do coexist at equilibrium, so that there is no thermodynamic driving force in one direction or the other. The system is thus inherently highly reactive with little intrinsic barrier.

Experimental Section

4′-Methoxy-3-methylflavylium perchlorate was synthesized in the normal way.[8b] Stock solutions ($2-4 \times 10^{-4}$ molar) were prepared in 0.01 M HCl.

Stopped-flow kinetic studies were performed on a Durrum-Gibson stopped-flow spectrophotometer thermostated at 25.0 °C. One syringe of the apparatus contained the stock flavylium ion solution mixed with an equal amount of 0.015 M NaOH to convert the cation into the *cis*-chalcone anion (see Results). The other syringe contained the appropriate buffer plus sufficient HCl to neutralize the excess hydroxide. The pH values of the solutions mixed on the spectrophotometer were recorded. The decrease in the signal at 295 nm was monitored. The photomultiplier output was digitized, with 120 points being recorded for each kinetic run. The digitized data were analyzed on a Tektronix 4051 microcomputer. Rate constants were evaluated as slopes of $\ln |A - A_\infty|$ vs. time. Five to eight kinetic runs were conducted for each solution. An accuracy of ±2% was found for solutions with a half-life greater than 20 ms, but a greater error was found for faster reactions, being of the order ±5% for a 6-ms half-life and ±10% for 2 ms.

Temperature-jump kinetic studies were performed on a Messanlangen-Studiengesellschaft spectrophotometer. The stock acid solution was mixed with the appropriate buffer, and sufficient sodium hydroxide was added to neutralize the acid. The pH of this solution was recorded, and the solution was placed in a *T*-jump cell. In several cases where dilute buffers were employed, the pH was recorded directly in the cell to check that there had been no change during the transfer. Unbuffered solutions were prepared by using CO_2-free doubly distilled water. The pH was adjusted by the addition of small amounts of 0.1 M NaOH and was recorded immediately before and immediately after the *T*-jump experiments. Some variation in pH was observed (up to 0.1 pH unit). The average of the two readings was taken. The spectrophotometer was thermostated at 21.5 °C and a 3.5 °C temperature jump applied. The monitoring wavelength was again 295 nm. The photomultiplier output was digitized with 380 points per run. Data analyses were carried out on an IBM 3033 computer (NEUCC, Copenhagen). Relaxation constants (τ^{-1}) were evaluated by least-squares fitting of the absorbance–time data to the exponential equation. Four to six kinetic runs were conducted for each solution. Accuracy is ±4% for solutions where the half-life is greater than 2 ms. The error increases for faster reactions and is ±8% for a half-life of 0.1 ms.

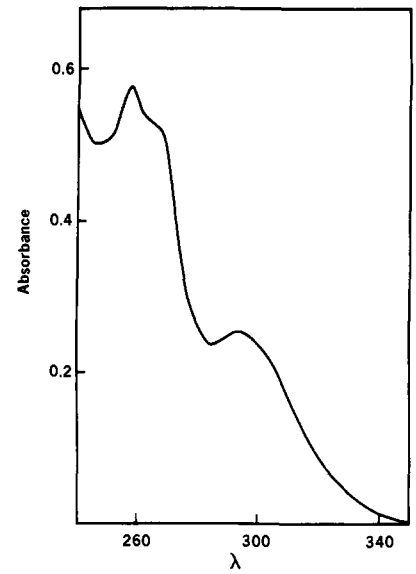

Figure 1. UV spectrum of a 1.4×10^{-4} M solution (pH 4.8).

Results

Equilibrium Constants. As will become apparent in the discussion, the following equilibria are important:

$$C \rightleftharpoons B \quad (3)$$

$$C \rightleftharpoons C^- + H^+ \quad (4)$$

$$B \rightleftharpoons B^- + H^+ \quad (5)$$

$$C^- \rightleftharpoons B^- \quad (6)$$

where C^- and B^- represent the deprotonated chalcone and hemiacetal, respectively. The equilibrium constant relating the neutral species, $K = [B]/[C]$, is 4 ± 0.4. This has been evaluated for the system of the present study[8b] with a method previously described.[7] The experiment involves the acidification to pH 1 of a neutral solution containing the equilibrium mixture of chalcone and hemiacetal. This results in conversion of both species to the 3-methyl-4′-methoxyflavylium ion. Since this occurs at different rates for the two compounds, the direct conversion involving the hemiacetal being faster, two kinetic phases are observed. The relative absorbance changes then provide the ratio of chalcone and hemiacetal.

At high pH the chalcone ionizes, displacing the equilibrium between the chalcone and hemiacetal toward the former. A pronounced increase in absorbance at 350 nm accompanies this process. When the absorbance at this wavelength is measured, a sigmoidal titration curve is obtained as a function of pH, giving an apparent acidity constant of $10^{-9.8}$. This constant is equal to $K_C/(1 + K)$,[9] where K_C is the true acidity constant for chalcone ionization. Substitution of the value for K provides $pK_C = 9.1 \pm 0.1$.

The acidity constant for hemiacetal ionization, K_B, cannot be measured. We estimate a value of 10^{-12}, based on literature values for other hemiacetals.[6b,10] A reasonable range for this estimate is ±0.5 pK unit. The K_B value provides the estimate $K^- = [B^-]/[C^-] = K_BK/K_C = 0.005$ for the final equilibrium in question, that involving the anionic forms.

(7) McClelland, R. A.; Gedge, S. *J. Am. Chem. Soc.* **1980**, *102*, 5838–5848.

(8) (a) No methyl on double bond. The substituents employed in this study were chosen because they avoid two other reactions common to this type of system,[7] loss of OH from the hemiacetal B in an acid-dependent equilibrium with a flavylium ion, and cis → trans isomerization of the double bond in the chalcone. In the present system[8b] the former reaction occurs only below pH 3.5 and the latter reaction at 25 °C apparently does not occur. (b) Devine, D. B.; McClelland, R. A. *J. Org. Chem.*, submitted. Devine, D. B., M.Sc. Thesis, University of Toronto, Toronto, 1982.

(9) If both chalcone ionization (K_C) and hemiacetal ionization (K_B) are considered, then the observed acidity constant is $(K_C + KK_B)/(1 + K)$. Since K_B is expected to be of the order of 10^{-12}, its contribution is unimportant.

(10) Formaldehyde hydrate, pK = 13.27: Bell, R. P.; Onwood, D. P. *Trans. Faraday Soc.* **1962**, *58*, 1557–1561. Benzaldehyde hydrate, $pK \approx 12.8$: Greenzaid, P. *J. Org. Chem.* **1973**, *38*, 3164–3167. 4-Nitrobenzaldehyde hydrate, pK = 12.1: Sayer, J. M. *J. Org. Chem.* **1975**, *40*, 2545–2547. α- and β-D-glucose, pK = 12.5 and 12.2, respectively: Los, J. M.; Simpson, L. B. *Recl. Trav. Chim. Pays-Bas* **1956**, *75*, 267–270. Trifluoroacetophenone hydrate, pK = 10.0: Stewart, R.; Van der Linden, R. *Can. J. Chem.* **1960**, *38*, 399–406. Cyclic hemiacetals of 2-(hydroxymethyl)benzaldehyde and 2-(β-hydroxyethyl)benzaldehyde, pK = 12.3: Harron, J.; McClelland, R. A.; Thankachan, C.; Tidwell, T. T. *J. Org. Chem.* **1981**, *46*, 903–910.

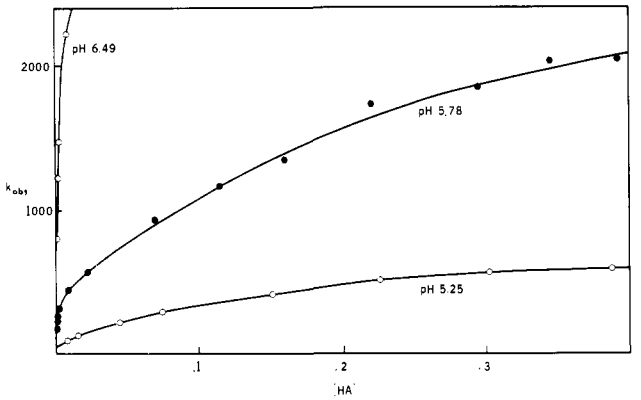

Figure 2. Rate constants in cacodylic acid buffers for chalcone–hemiacetal equilibration at 25 °C and ionic strength 0.5. [HA] is the concentration of the acid component of the buffer. Rate constants at pH 6.49 and 5.78 were obtained by the temperature-jump method and those at pH 5.25, by the stopped-flow method. Lines drawn are the best lines joining the points.

Stopped-Flow Kinetics. These were carried out by taking advantage of the displacement in base of the equilibrium in question. Reacidification of a base solution to neutral pH restores the equilibrium between the two neutral forms, and that return to equilibrium can be monitored. We observed the decrease in absorbance at 295 nm, associated with the decrease in concentration of the excess *cis*-chalcone (see next section for discussion of UV spectrum).

Temperature-Jump Kinetics. A significant relaxation is observed when a temperature jump from 21.5 to 25.0 °C is applied to an equilibrating solution of the chalcone and hemiacetal. The UV spectrum of this solution (Figure 1) has an absorption band with λ_{max} at 295 nm, which we interpret as belonging to the *cis*-chalcone. A stronger absorption with λ_{max} at 260 nm is also seen. This is probably due to the hemiacetal although the chalcone may contribute here as well. The temperature jump produces an absorbance increase at 295 nm of about 0.008 absorbance unit for a 1.4×10^{-4} M solution (total concentration), and this was used to obtain relaxation constants. This change corresponds to an increase in the equilibrium chalcone concentration with increasing temperature. A small decrease in absorbance of about 0.002 unit is observed at 260 nm. This corresponds to a decrease in hemiacetal concentration, and the observation that it is occurring in the direction opposite to that at 295 nm is good evidence that these relaxations do represent the chalcone–hemiacetal equilibration.

Rate Constants. The two techniques were used to obtain rate constants in cacodylic acid buffers of pH 5.2–6.5 (Table S1). Figure 2 depicts plots of rate constant vs. buffer concentration for three pH values. The temperature-jump method has two advantages. It can be used at higher pH where the relaxation is too rapid for the stopped-flow method. Moreover it permits the use of solutions of very low buffer concentrations. Because of the requirement for neutralizing the base in the stopped-flow method, we experienced problems controlling the pH in very dilute buffers using this method. With the temperature-jump method, the pH of the solution in question can be measured and adjusted if necessary.

The temperature-jump method was also applied to a series of solutions with no buffer and pH between 5.4 and 7.3 (Table S2). These relaxation constants were found to be linear in hydroxide ion concentration[11] with $k_{obsd}/[OH^-] = (5.8 \pm 0.8) \times 10^9$ M^{-1} s^{-1}.

Discussion

We interpret the rate–buffer curves as having three regions of behavior: very dilute buffers, where the rate rises very rapidly; dilute to moderately concentrated buffers, where the rate continues to increase as buffer is added but not nearly so steeply; and concentrated buffers, where the rate levels and becomes independent of buffer concentration. Breaks in linearity in buffer dilution plots are usually interpreted as indicating a change in rate-limiting step.[12] The plots of this system exhibit two breaks, implying therefore two changes and at least three steps in the reaction. There are however at most three steps, one C–O bond-making/bond-breaking step and two proton-transfer steps, and we propose therefore that all three are separate and that both the chalcone anion and hemiacetal anion are intermediates.

$$C \xrightarrow[k_{-1}^0 + k_{-1}^H[H^+] + k_{-1}^{HA}[HA]]{k_1^{OH}[OH^-] + k_1^0 + k_1^A[A^-]} C^- \underset{k_{-2}}{\overset{k_2}{\rightleftharpoons}} B^- \xrightarrow[k_{-3}^{OH}[OH^-] + k_{-3}^0 + k_{-3}^{HA}[HA]]{k_3^0 + k_3^H[H^+] + k_3^{HA}[HA]} B \quad (7)$$

The interconversion of the two anions obviously occurs with no catalysis (eq 8). The equilibrium constant K^- is equal to k_2/k_{-2}

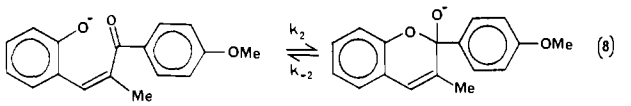

(8)

and since K^- is less than one, k_2 must be less than k_{-2}. Each proton transfer can occur with three acids or bases, including the solvent (k^0 terms) and the buffer. Relationships 9 and 10 apply, where

$$K_C = \frac{k_1^0}{k_{-1}^H} = \frac{k_1^{OH}K_w}{k_{-1}^0} = \frac{k_1^A K_{HA}}{k_{-1}^{HA}} \quad (9)$$

$$K_B = \frac{k_{-3}^0}{k_3^H} = \frac{k_{-3}^{OH}K_w}{k_3^0} = \frac{k_{-3}^A K_{HA}}{k_3^{HA}} \quad (10)$$

K_w is the autoprotolysis constant[11] and K_{HA} is the cacodylic acid acidity constant ($10^{-6.1}$). From the known K_C and estimated K_B, estimates can be made for these constants. Thus k_1^{OH}, k_{-3}^{OH}, k_{-1}^H, k_3^H, k_{-1}^{HA}, and k_3^{HA} represent proton transfers in the thermodynamically favored direction and should have values near 10^{10} M^{-1} s^{-1}. Then from eq 9 and 10, $k_{-1}^0 \approx 10^5$ s^{-1}, $k_3^0 \approx 10^8$ s^{-1}, $k_1^0 \approx 10^1$ s^{-1}, $k_{-3}^0 \approx 10^{-2}$ M^{-1} s^{-1}, $k_1^A \approx 10^7$ M^{-1} s^{-1}, and $k_3^A \approx 10^4$ M^{-1} s^{-1}. From these numbers it can be seen that at pH >5.3 both proton-transfer steps in the absence of buffer proceed predominantly with deprotonation by hydroxide or protonation by water, so that in the kinetic analysis the terms in k_1^0, k_{-1}^H, k_{-3}^0, and k_3^H are neglected. We also define $k_1 = k_1^{OH}[OH^-] + k_1^A[A^-]$ and k_{-1}, k_3, and k_{-3} similarly, these representing the first-order proton-transfer rate constants in a particular kinetic experiment.

$$C \underset{k_{-1}}{\overset{k_1}{\rightleftharpoons}} C^- \underset{k_{-2}}{\overset{k_2}{\rightleftharpoons}} B^- \underset{k_{-3}}{\overset{k_3}{\rightleftharpoons}} B \quad (11)$$

A relaxation treatment[13] can then be applied to eq 11, producing three relaxation constants, which cannot be separated. A simplification can however be introduced since at pH <7 only the neutral species C and B are present in significant concentration, requiring $k_1 < k_{-1}$ and $k_{-3} < k_3$ and producing eq 12.[14] The latter

$$k_{obsd} = \frac{k_1k_2k_3 + k_{-1}k_{-2}k_{-3}}{k_{-1}k_{-2} + k_{-1}k_3 + k_2k_3} = \left(\frac{1+K}{K}\right)\frac{k_1k_2k_3}{k_{-1}k_{-2} + k_{-1}k_3 + k_2k_3} \quad (12)$$

expression in eq 12 arises since $k_1k_2k_3/(k_{-1}k_{-2}k_{-3}) = K$. It can also be noted that the rate constant in the forward direction is $k_1k_2k_3$ divided by the denominator in eq 12, and that for the

(11) (a) Hydroxide ion concentrations were calculated by using $pK_w = 13.7$.[11b] (b) Harned, H. S.; Owen, B. B. "The Physical Chemistry of Electrolytic Solutions", 3rd ed.; Reinhold: New York, 1958.

(12) Jencks, W. P. "Catalysis in Chemistry and Enzymology"; McGraw-Hill: New York, 1968; p 465.

(13) Bernasconi, C. F. "Relaxation Kinetics", Academic Press: New York, 1976.

(14) A detailed derivation of all kinetic equations is given as supplementary material.

(15) Little difference in the statistics of the fit was observed whether the constant A was fixed or allowed to vary.

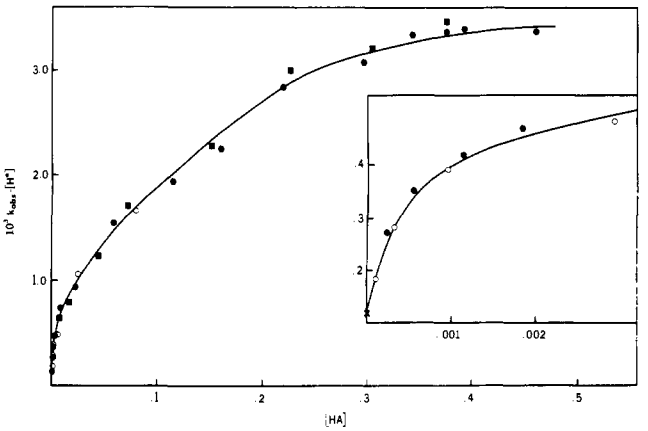

Figure 3. Rate constants multiplied by the proton concentration as a function of the concentration of cacodylic acid: (■) pH 5.25; (●) pH 5.78; (○) pH 6.49; (×) value of coefficient A obtained from kinetic data with no added buffer. Lines drawn are based on eq 13 and values of the coefficients A–E are listed in Table I.

Table I. Rate and Equilibrium Constants for Chalcone–Hemiacetal Equilibrium

constant	source	value	range
K	meas	4	3.6–4.4
pK_C	meas	9.1	9.0–9.2
pK_B	est	12	12.5–11.5
K^-	K_BK/K_C	0.005	0.002–0.02[a]
A	rate data, no buffer	1.2×10^{-4}	$(1.0–1.4) \times 10^{-4}$
B	least squares fit to eq 13 with A fixed	3	1.5–4.5[b]
C		60	55–65[b]
D		3×10^3	$(2.5–3.5) \times 10^5$ [b]
E		1.1×10^4	6×10^3–1.6×10^4 [b]
k_1^{OH}, M^{-1} s^{-1}	rate data, no buffer	6×10^9	$(5–7) \times 10^9$
k_{-1}^0, s^{-1}	A/K_C	1.5×10^5	$(1.2–1.8) \times 10^5$
k_1^A, M^{-1} s^{-1}	B/K_{HA}	4×10^6	$(2–6) \times 10^6$
k_{-1}^{HA}, M^{-1} s^{-1}	B/K_C	4×10^9	$(2–6) \times 10^9$
k_2, s^{-1}	$CK/(EK_C(1 + K))$	6×10^6	3×10^6–1×10^7
k_{-2}, s^{-1}	k_2/K^-	1×10^9	3×10^8–3×10^9 [a]
k_3^0, s^{-1}	$B/(DK_B(1 + K))$	1×10^8	2×10^7–5×10^8 [a]
k_{-3}^{OH}, M^{-1} s^{-1}	$B/(DK_w(1 + K))$	7×10^9	4×10^9–1.4×10^{10}
k_3^{HA}, M^{-1} s^{-1}	$C/(DK_B(1 + K))$	4×10^9	1×10^9–2×10^{10} [a]
k_{-3}^A, M^{-1} s^{-1}	$C/(DK_{HA}(1 + K))$	4×10^3	$(3–5) \times 10^3$

[a] Range determined by uncertainty in K_B estimate. [b] Based on standard deviations determined from multiparameter fit.

reverse direction is $k_{-1}k_{-2}k_{-3}$ divided by the same denominator. Substitution of the appropriate expressions for k_1 etc. into eq 12 produces eq 13. With some simplifying assumptions based on

$$k_{obsd} = \frac{1}{[H^+]} \frac{A + B[HA] + C[HA]^2}{1 + D[HA] + E[HA]^2} \qquad (13)$$

the expected magnitudes of various rate constants,[14] the coefficients are $A = k_1^{OH}K_w$, $B = k_1^AK_{HA}$, $C = K_{HA}k_1^Ak_3^{HA}/k_3^0$, $D = (K/(1 + K))(K_{HA}K^-k_1^A/K_Ck_3^0)$, and $E = (K/(1 + K))(K_{HA}k_1^Ak_3^{HA}/K_Ck_2k_3^0)$. Equation 13 predicts that a plot of $k_{obsd}[H^+]$ vs. [HA] should result in a common curve independent of pH (or buffer ratio), and this is found (Figure 3). The analysis also predicts the dependency on hydroxide ion concentration observed in the absence of buffer. These experiments also provide $k_1^{OH} = 6 \times 10^9$ M^{-1} s^{-1} and $A = 1.2 \times 10^{-4}$. This leaves four variables unknown in eq 13 and a least-squares fit was conducted to give their values. Appropriate algebraic manipulations then provide all individual rate constants. These are summarized along with estimates of their precision in Table I. It can be noted that those

Table II. Values of Rate Constants in a Cacodylic Acid Buffer pH 5.78

[HA]	k_{-1}	k_3	$k_{-1}k_{-2}$	$k_{-1}k_3$	k_2k_3
0	1.5×10^5	1.0×10^8	1.5×10^{14}	1.5×10^{13}	6.0×10^{14}
0.00004	2.7×10^5	1.0×10^8	2.7×10^{14}	2.7×10^{13}	6.0×10^{14}
0.0001	4.5×10^5	1.0×10^8	4.5×10^{14}	4.5×10^{13}	6.0×10^{14}
0.0002	7.5×10^5	1.0×10^8	7.5×10^{14}	7.6×10^{13}	6.0×10^{14}
0.0005	1.7×10^6	1.0×10^8	1.7×10^5	1.7×10^{14}	6.1×10^{14}
0.001	3.2×10^6	1.0×10^8	3.2×10^{15}	3.3×10^{14}	6.2×10^{14}
0.004	1.2×10^7	1.2×10^8	1.2×10^{16}	1.4×10^{15}	7.0×10^{14}
0.01	3.0×10^7	1.4×10^8	3.0×10^{16}	4.2×10^{15}	8.4×10^{14}
0.04	1.2×10^8	2.6×10^8	1.2×10^{17}	3.1×10^{16}	1.6×10^{15}
0.10	3.0×10^8	5.0×10^8	3.0×10^{17}	1.5×10^{17}	3.0×10^{15}
0.25	7.5×10^8	1.1×10^9	7.5×10^{17}	8.3×10^{17}	6.6×10^{15}
0.60	1.2×10^9	1.7×10^9	1.2×10^{18}	2.0×10^{18}	1.0×10^{16}

constants whose values depend on K_B have a large range because of the uncertainty of this value. The other constants are independent of K_B and are therefore determined more precisely, although even with these the ranges are large because of uncertainties introduced by the multiparameter fit. Significantly however the proton-transfer rates do lie within the ranges predicted on the basis of acidity constant considerations. It is interesting in this respect that k_3^{HA} is predicted as 4×10^9 M^{-1} s^{-1}, as expected for a proton transfer in the thermodynamically favored direction. The value of this constant does depend on the K_B estimate, and the agreement implies that the estimate cannot be greatly in error. For example a pK_B of 10.5 would result in a k_3^{HA} value of 10^8 M^{-1} s^{-1}, well below the 10^{10} value expected, while a pK_B of 13.5 would produce k_3^{HA} equal to 10^{11} M^{-1} s^{-1}.

Also of importance is the finding that $k_2 > k_{-1}^0$ and $k_{-2} > k_3^0$, since these two relationships are responsible for the complex rate behavior. In simple terms, the anions C^- and B^- interconvert in the absence of buffer more rapidly than either is protonated, so that the interconversion cannot be rate limiting. The addition of buffer however accelerates the proton-transfer rates so that the changes in rate-limiting step can occur. A detailed analysis can be conducted by noting that the question of rate-limiting step is determined by the relative magnitudes of the three terms in the denominator of eq 12. For example, when k_2k_3 is greater than both $k_{-1}k_{-2}$ and $k_{-1}k_3$, the expression for k_{obsd} collapses to $(1 + K/K)k_1$, and the first step is rate limiting. Similarly, when $k_{-1}k_{-2}$ or $k_{-1}k_3$ dominates, the third step or second step, respectively, is rate limiting. Values of these three terms calculated from the rate constants in Table I are listed in Table II. As predicted from the two breaks in the buffer dilution plots, at some concentration of buffer each step in the reaction is rate limiting (or mainly rate limiting)—the first step in very dilute buffers, then the third step, and finally the second step in concentrated buffer. In this extreme both proton transfers have become fast because of the reaction with the buffer, so that $k_2 < k_{-1}$ and $k_{-2} < k_3$ and the rate is independent of buffer, since it no longer participates in the rate-limiting step. The differential effect of buffer on k_{-1} and k_3 (see Table II) is responsible for the shift in dilute buffers from a rate-limiting first step to a rate-limiting third step. This effect arises since $k_{-1}^0 \ll k_3^0$ while $k_{-1}^A \approx k_3^A$ so that the added buffer can affect the k_1 rate in much more dilute solutions than it can affect the k_3 rate.

In some respects the complex rate behavior is a consequence of the equilibrium nature of this system, so that the various rate constants are related. A more simple way of looking at the kinetics is as follows. In no buffer and very dilute buffers where $k_{-1} < k_2$ and $k_3 < k_{-2}$, the rate-limiting step is that with the slowest anion protonation, the first step. As a consequence of the differential effect of buffer on k_{-1} and k_3, $k_{-1} > k_2$ in quite dilute buffers ($\approx 10^{-3}$ M) and the first step therefore can no longer be rate limiting. However, k_3 is still less than k_{-2} so the change is to the third step. In concentrated buffers k_3 becomes greater than k_{-2}, and a further change occurs to rate-limiting second step.

Summary

A comparison of this system with those of other acetals reveals two interesting differences. First, both proton transfers here are

separate from C–O bond making or breaking, so that there is no concerted proton transfer during this step.[16] Second, both C–O bond making and C–O bond breaking are extremely rapid, so rapid that in dilute buffers proton-transfer steps are rate limiting, and in fact buffer catalysis is still observed. The actual complex kinetic pattern is also interesting. As far as we are aware this is the first example where two changes in the rate-limiting step occur as the buffer concentration is changed.[17]

The uncoupling of both proton transfers in the present case is undoubtedly a consequence of the significantly more stable anionic leaving group or nucleophile. In this respect it is interesting to consider at which point this uncoupling will occur. In the detailed studies of formaldehyde hemiacetals[1] and acetaldehyde hemiacetals,[3] the most stable alkoxide was that derived from the hemiacetals of trifluoroethanol, $pK_a = 12.4$.[18] Interestingly, these hemiacetals still apparently follow the general mechanistic behavior of eq 1 in their base decomposition, despite the fact that the alkoxide is now at least as stable as the hemiacetal anion.[19] It appears that the mechanistic changeover occurs for alcohols/phenols somewhere between trifluoroethanol and the chalcone of this study. (The structure of the carbonyl component is undoubtedly also important. What is needed is a study of a set of hemiacetals derived from a common aldehyde or ketone. It should also be noted that the reaction of the present study is intramolecular, and this could have significant effects.)

The chalcone system is also interesting in that the hemiacetal anion, now the less stable anion, still forms as a discrete intermediate. This is in contrast to the trifluoroethyl hemiacetal systems where the stability of the two anions as reflected by acidity constants is close and yet one of the anions is avoided. The chalcone hemiacetal anion does however have a very short lifetime with respect to C–O bond cleavage. With even more stable leaving groups the situation can be imagined where the hemiacetal anion would not have a sufficient lifetime to exist at all.[20] The reaction would then return to a two-step mechanism (class e), now with the hemiacetal anion being avoided by concerted proton transfer.

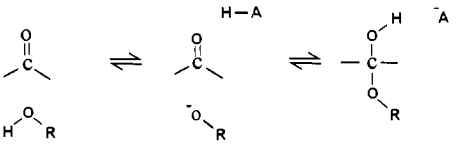

A possible example of this is the reversible cyclization of the *o*-formylbenzoate anion,[21,22] where the nucleophile/leaving group is a very stable carboxylate.

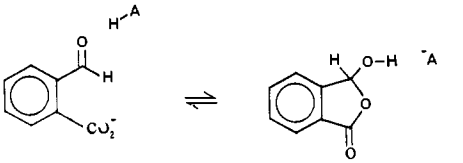

Acknowledgment. The financial support of the Natural Sciences and Engineering Research Council of Canada is gratefully acknowledged. We also thank Statens Naturvidenskabelige Forskningsraad for an equipment grant.

Supplementary Material Available: Kinetic derivation for eq 13 and tables of rate constants with and without buffers (7 pages). Ordering information is given on any current masthead page.

(16) With hemiacetals derived from simple alcohols the possibility does exist[1-3] that the hydroxide ion catalyzed breakdown involves three steps and a discrete alkoxide intermediate; it is the catalysis by other bases that involves the two-step mechanism of eq 1.

(17) See McClelland (McClelland, R. A. *J. Am. Chem. Soc.* **1984**, *106*, 7579–7583) for an example where changes in buffer concentration result in a single change in rate-limiting step in the breakdown of a hemi-ortho ester, from a proton-transfer step in dilute buffers to C–O bond breaking in more concentrated buffers.

(18) Ballinger, P.; Long, F. A. *J. Am. Chem. Soc.* **1959**, *81*, 1050–1053.

(19) The pK_a values for the trifluoroethyl hemiacetals of formaldehyde and acetaldehyde are estimated as 12.85[1] and 13.14,[3] respectively. The fact that Brønsted β coefficients for the base-catalyzed decomposition of these two substrates (0.58 for formaldehyde[1] and 0.73 for acetaldehyde[3]) are still considerably lower than unity (although approaching this value) indicates that the mechanism is probably still concerted.

(20) Jencks, W. P. *Acc. Chem. Res.* **1980**, *13*, 161–169.

(21) Bell, R. P.; Cox, B. G.; Timimi, B. A. *J. Chem. Soc. B* **1971**, 2247–2250.

(22) Sørensen, P. E.; McClelland, R. A., in preparation.